J Mater Sci (2010) 45:5339–5346
DOI 10.1007/s10853-010-4582-5

Effect of cold rolling on microstructure and magnetic properties in a metastable lean duplex stainless steel

Silvia Baldo · Istvan Mészáros

Received: 28 March 2010 / Accepted: 28 April 2010 / Published online: 14 May 2010

Abstract Microstructural and magnetic properties changes of a metastable ferritic–austenitic stainless steel due to cold rolling were studied together with the possibility to develop a new ferritic–martensitic stainless steel. In order to reduce costs low-Ni content was maintained in the lean duplex stainless steel considered, making it more susceptible to strain-induced martensitic transformation. In this study a practically complete $\gamma \rightarrow \alpha'$ transformation was found for 80% of thickness reduction, resulting a new two-phase ferritic–α' martensitic stainless steel. To investigate the structural evolution different values of thickness reduction were applied. Light optical and scanning electron microscopy were performed to characterize the morphology and grain refining of the structure after each rolling step. Martensitic transformation and work hardening were detected and analyzed by studying of magnetic properties (saturation magnetic polarization, relative magnetic permeability, coercivity). Additionally, hardness tests were performed. The results highlighted a strong grain refining and increase in martensitic phase and hardness with increasing cold deformation. A direct relationship between microstructure and magnetic properties was revealed. In particular the reciprocal of relative magnetic permeability and the coercivity increased with martensite content and the amount of cold deformation. Therefore, the possible application of magnetic measurements as non-destructive tests to study microstructural evolution during cold rolling was shown for the steel considered.

S. Baldo (✉)
Department of Engineering's Chemical Processes (DPCI), University of Padova, Via Marzolo 9, 35131 Padova, Italy
e-mail: silvia.baldo@unipd.it

I. Mészáros
Department of Material Science and Engineering, Budapest University of Technology and Economics (BUTE), Budapest, Hungary

Introduction

In the last decades, the development of low-cost stainless steels has been carried out to reduce the cost fluctuation of certain expensive elements such as Ni and Mo. Austenitic stainless steels were partly substituted by ferritic–austenitic duplex stainless steels, characterized by comparable corrosion resistance, better mechanical properties, and less content of Ni and Mo. However, the requirement of high-strength steels with good corrosion resistance can be satisfied with a new type of two-phase stainless steel. Hayden and Floreen [1] studied the influence of martensite and ferrite on the properties of a ferritic–martensitic stainless steel. In their study, martensite is obtained by cooling at high subzero temperatures as dispersed islands in a ferritic matrix. The results highlighted the beneficial effects of martensite on mechanical resistance and toughness. In this study, the possibility to create a new ferritic–martensitic stainless is studied. Hence, cold deformation is applied on ferritic–austenitic lean duplex stainless steel to obtain a ferritic–martensitic stainless steel with strain-induced martensite in a ferritic matrix.

With the aim to improve both mechanical and surface properties for structural applications, cold rolled finishes can be applied to flat products. The main effects of cold rolling are to smooth the material surface, to refine the grain structure, and sometimes to induce microstructural changes. Many authors have investigated the formation of strain-induced martensite due to plastic deformation mainly in AISI 301, 304, and 316 austenitic stainless steels [2–9] and common duplex stainless steels [10]. In the latest

years, new ferritic–austenitic duplex stainless steels were get ready [11, 12]. These new types of duplex stainless steels are characterized by a further decrease in Ni, substituted by Mn and sometimes by N, leading to a higher instability of austenitic phase that can evolve to martensite after cold deformation or heat treatment. It is well known that two types of martensite can form from metastable austenite: ε hcp paramagnetic and α' bcc ferromagnetic martensite. The α' is thermodynamically more stable than ε martensite. The ε phase forms before the α' phase and increasing deformation α' grows at the ε phase expense. Finally, at high deformation α' martensite predominates. Based on these observations the sequence of transformation $\gamma \rightarrow \varepsilon + \alpha'$ was suggested [4, 8]. The diffusionless transformation from γ-phase, paramagnetic, into α' phase, strongly ferromagnetic, can be detected by studying the magnetic properties of the deformed material.

Actually there is a growing interest in the use of magnetic measurements as non-destructive evaluation techniques for monitoring the strain-induced martensite transformation in steels characterized by metastable austenitic phase.

In this study, the microstructural changes produced by cold rolling in a ferritic–austenitic lean duplex stainless steel have been investigated. A lean duplex stainless steel with low content of metastable austenite has been chosen in order to obtain a final structure characterized only by ferrite and strain-induced martensite. The effect of cold rolling on microstructure and grain refining has been investigated through metallographic technique using light optical and scanning electron microscopy. Magnetic measurements and X-ray diffraction (XRD) have been performed to assess the amount of strain-induced martensite after cold rolling with different thickness reductions.

Finally Vickers microhardness and coercivity measurements have been carried out for each step of cold rolling.

Experimental

The material under investigation was a lean duplex stainless steel (chemical composition shown in Table 1) received as hot rolled plates of 8 mm in thickness, solution annealed at 1050 °C for 30 min, and then quenched in water. Plastic deformation of the solution annealed material was carried out by cold rolling at ambient temperature. A single stand reversing mill with 130-mm diameter rolls was used. The plates were cold rolled in one direction, through many constant passes, to gradually reduce its thickness by compression. A thickness reduction of 0.10 mm was used for each pass, in order to perform high cold deformation without strong bending. Seven cold rolled samples were obtained applying different thickness reductions in the range 10–80%.

Table 1 Chemical composition of the stainless steel studied in this study (wt%)

C	Cr	Mn	Ni	Si	Mo	P	S	N	Cu	Fe
0.028	21.72	3.41	1.13	0.78	0.15	0.026	0.01	0.13	0.32	Bal.

Metallographic samples were prepared by conventional grinding, polishing, and etching with Beraha's etchant. Microstructural investigations were carried out using a light optical microscope (Leica DMRE) on etched samples and scanning electron microscopy (Stereoscan 440 SEM, Cambridge) using the backscattered electron (BSE) signal on unetched samples. In particular the BSEs detector was set to maximize the atomic number contrast, allowing ferrite, austenite, and other phases to be detected. Quantitative metallography was performed using Leica QWin image software analysis. The volume fractions of austenite and ferrite in the solution annealed material were determined on three longitudinal and three transversal sections (20 fields for each section) on light optical micrographs at 200×, after etching with Beraha's metallographic reagent.

For the identification of the phases, XRD was performed in a diffractometer Siemens® D500 XRD using a Cr Kα radiation ($\lambda = 2.2897$ Å, operating at 30 kV and 20 mA), in step scan mode with step size of 0.025° and time per step of 5 s. The diffractograms have an angular range 50–120°.

First magnetization curve and hysteresis loops were measured in a double-yoke DC magnet-steel tester. The predecessor equipment was firstly described by Stäblein and Steinitz. Our equipment is characterized by two E-shaped soft iron yokes, opposite one another with an air-gap between each of the three pairs of transverse limbs. Equal magnetizing windings are placed on each half of the long arms of both yokes. Hence, the equipment has a perfect symmetry. The introduction of a specimen in one gap causes an imbalanced symmetry; an additional flux is needed to complete the circuit mainly across the central air-gap, the flux in which is thus closely proportional to the magnetization (M) of the specimen. The apparatus for measuring the strength of the applied field H may be calibrated in any known field, and is found to give accurate readings of the value of H applied to the specimen [13]. The maximum applied external field was of 210 kA/m. The present form of the measuring setup is developed at the Department of Materials Science and Engineering of the BUTE and it applies up to date field sensors and data acquisition apparatus. AC measurements of the minor hysteresis loops were carried out by using a specifically designed permeameter type magnetic property analyzer, with a maximum applied external field of 2450 A/m. For

each cold rolled sample the relative magnetic permeability values were derived from the resulting magnetizing curves. The coercivity (H_c) was measured by a high-accuracy Förster coercimeter (Type 1.093) equipment, based on the compensation of the own remnant magnetic field of the samples. The coercivity was measured magnetizing the samples along their rolling direction. Vickers hardness (HV) tests were also performed using a Buehler MMT-3 digital microhardness tester. All measurements were carried out using a load of 0.5 kg on each sample.

Results and discussion

Microstructural observations

The as-received material in the solution annealed condition is characterized by coarse austenitic grains in a ferritic matrix. Austenitic grains are elongated in longitudinal direction due to the previous hot rolling (Fig. 1a, b) and equiassic in the transversal cross section, perpendicular to rolling direction (Fig. 1c). The measured average volume fraction of austenite and ferrite is of 20.4 and 79.6, respectively.

The first effects obtained by cold rolling were the strong grain refining and changing in shape compared to the solution annealed sample microstructure. The grain refining is a consequence of elongation and break of grains due to deformation at room temperature. Particularly with intermediate stage of thickness reductions (Fig. 2) grain refining and flattening began to be evident in the section perpendicular to cold rolling direction, whereas a higher elongation and width reduction of austenitic grains were detected in the direction of cold rolling (Fig. 3).

By increasing strain to the maximum value considered in this study, a stronger grain refinement was revealed in all the sections of the samples (Fig. 4a, b). The average value of flattening in austenitic grains changed of about 80%: from a grain height of almost 10 μm in the as-received material to almost 2 μm in the higher thickness reduction applied (Figs. 1c and 4b).

The other important effect obtained to cold rolling is the strain-induced martensitic transformation. The quantification of martensitic phase was not possible through classical metallographic technique because Beraha's etchant unequivocally was able to distinguish only the ferritic (dark) and the austenitic (light) phase.

The micrographs obtained by SEM using BSE signal highlighted some fluctuations of color inside the austenitic grains after cold deformation, due to local differences in chemical composition but did not clearly reveal the presence of a different martensitic phase. Hence, martensitic phase is believed to have almost the same chemical composition of its parent austenitic phase.

XRD and magnetic measurements

XRD and magnetic measurements were so performed for the identification and quantification of α'-martensite for each thickness reduction in cold rolled samples.

In Fig. 5 X-ray diffractograms of solution annealed sample without cold deformation (0% thickness reduction) and of the strongest deformed sample (80% thickness reduction) are shown.

In the cold rolled samples the peaks of ferrite (δ) and α'-martensite are not distinguishable as the two phases present the same reflections. Over the detection limit the peak of austenitic phase completely disappears after the maximum thickness reduction applied. Therefore, it can be

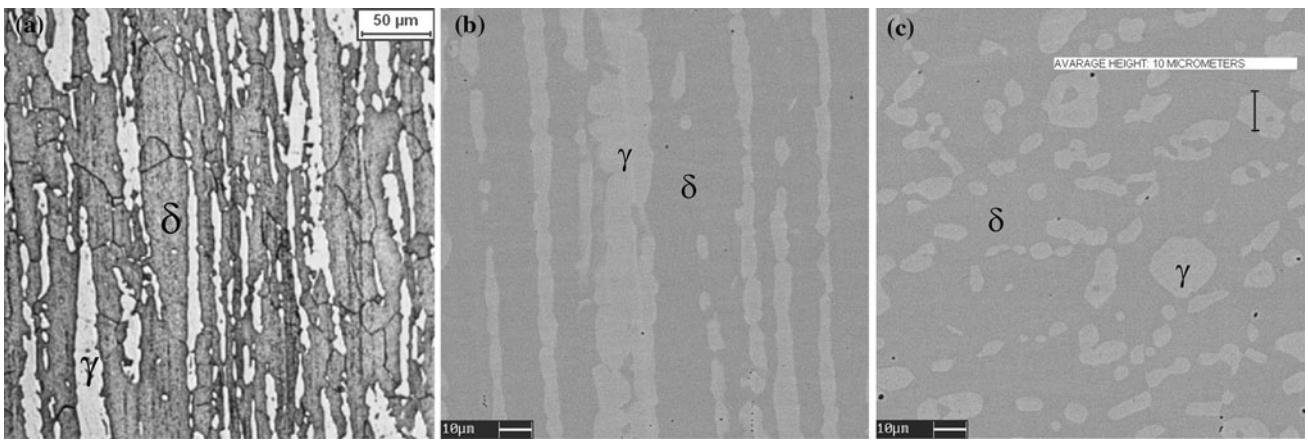

Fig. 1 As-received material of **a** Beraha's etching, light optical micrograph, **b** longitudinal section, SEM–BSE micrograph, **c** transversal section, SEM–BSE micrograph

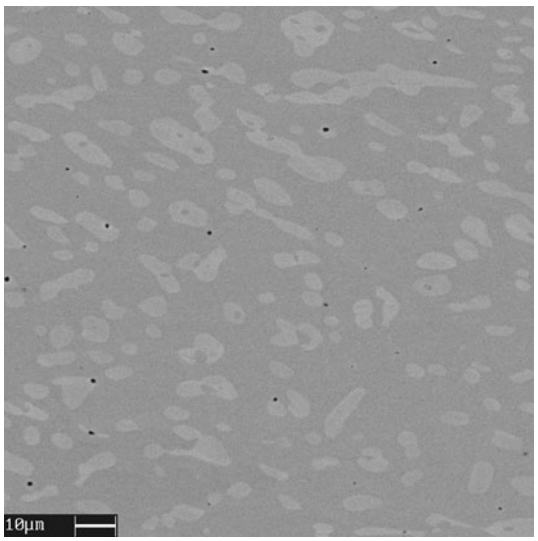

Fig. 2 Cold rolled material thickness reduction 40%, transversal section, SEM–BSE micrograph

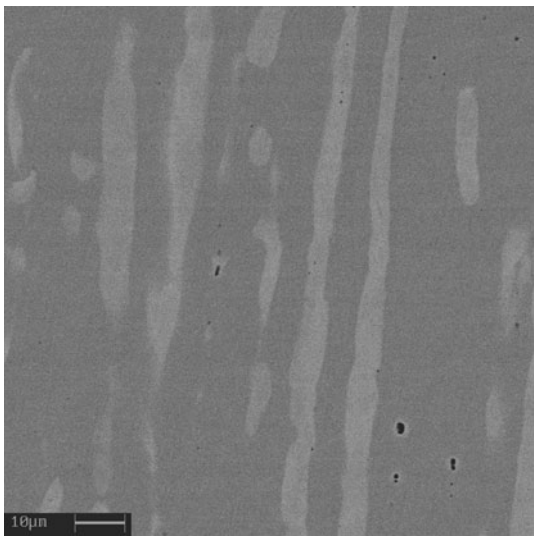

Fig. 3 Cold rolled material thickness reduction 50%, longitudinal section, SEM–BSE micrograph

concluded that at this deformation condition all the austenitic phase detectable transformed into α'-martensite. This last result together with phase quantification previously performed through image analysis leads to calculate the amount of ferromagnetic α'-martensite in each cold rolled sample. The saturation magnetic polarization is in fact linearly proportional with the amount of ferromagnetic phase. In the non-deformed condition only a ferromagnetic phase (δ-ferrite) was present in a structure characterized by 79.6% of ferrite and 20.4% of austenite. The saturation magnetic polarization in this case was $\mu_0 M_s\,(\delta) = 0.752$ T, and remained a constant value during cold rolling. With the application of cold deformation another ferromagnetic component was introduced because of the appearance of α'-martensite, which increased with cold deformation up to a complete detectable ferromagnetic structure made of 79.6% of ferrite, 20.4% of α'-martensite and 0% of austenite. The relation between saturation magnetic polarization $\mu_0 M_s$ and the amount of ferromagnetic phase was

$$\mu_0 M_s = \mu_0 M_s(\delta) + a \cdot \alpha'(\%),$$

where $\mu_0 M_s\,(\delta)$ was the saturation magnetic polarization of ferrite and $\alpha'(\%)$ was the amount of α'-martensite. The slope (a) of the line was determined (Fig. 6a) knowing the saturation magnetic polarization values in the non-deformed sample and in the fully ferromagnetic sample. Therefore, it was possible to calculate the amount of α'-martensite, $\alpha'(\%)$, corresponding to each value of saturation magnetic polarization and thickness reduction (Fig. 6a).

The saturation magnetic polarization ($\mu_0 M_s$) seems to be almost the same at lower thickness reduction (up to 30%) (Fig. 6b). Further increase in cold deformation has the consequence of stronger and gradual increase in saturation magnetic polarization due to the increasing presence of ferromagnetic α'-martensite, reaching the highest value of 0.94 T for the highest thickness reduction imposed (80%).

Relative magnetic permeability and maximal relative permeability values were derived from AC normal magnetization curves (Fig. 7a, b). As it is well known that the normal magnetization curve is the locus of the peak points of symmetrical minor hysteresis loops and the magnetic permeability is the slope of the normal magnetization curve. Magnetic permeability is an index of how well a material concentrates the magnetic field. In austenitic stainless steels cold rolling induces an increasing of relative permeability [14], corresponding to an increase in ferromagnetic α'-martensite content. In contrast to austenitic stainless steels, the duplex stainless steel investigated in this study shows an inverse ratio between relative permeability and cold deformation. Probably this is due to the appearance of ferromagnetic strain-induced martensite and to the interaction between dislocations introduced by cold rolling and magnetic domain walls in the ferritic phase [15]. Therefore, the results show a relationship between the reciprocal of maximum relative magnetic permeability and the presence of strain-induced martensite, making relative magnetic permeability a possible non-destructive measurement to detect martensitic transformation in the duplex stainless steel considered.

Vickers hardness and coercivity measurements

The results of Vickers hardness and coercivity H_c are plotted together with the thickness reduction of the samples in Fig. 8. Both Vickers hardness and H_c linearly increase

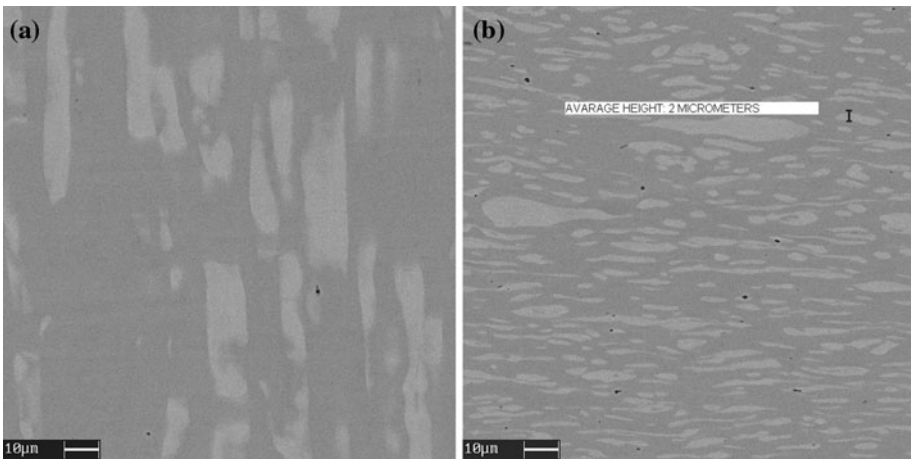

Fig. 4 Cold rolled material thickness reduction 80% of **a** longitudinal section SEM–BSE micrograph, **b** transversal section, SEM–BSE micrograph

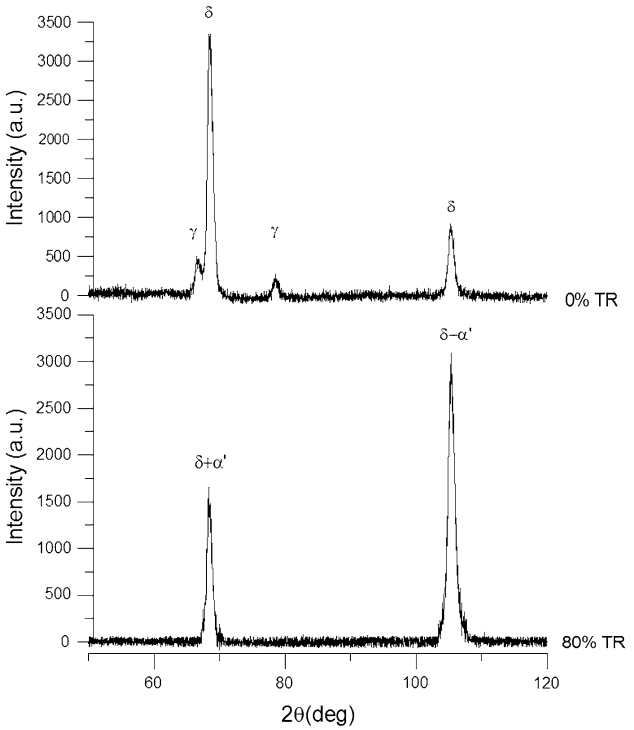

Fig. 5 X-ray diffractogram of as-received material and cold rolled material (80% thickness reduction)

with cold deformation, but with different trends. According to saturation magnetic polarization values the principal phenomenon at low strain rates is strain hardening so Vickers hardness rapidly increases up to 20% of thickness reduction. For further deformations martensitic transformation takes place, reflecting a slight decrease in the slope of hardness curve and strong increase of H_c.

H_c is an extrinsic property of materials, sensitive to microstructural conditions, and it usually increases with the dislocation density and the reciprocal of grain size [16].

Some authors [17, 18] have studied the variation of coercivity H_c due to cold deformation in metastable austenitic stainless steels, finding different connections revealing different mechanism of ferromagnetism in dependence of low and high content of α'-martensite. In some studies H_c reaches a saturation value after cold deformation [18], in other works H_c decreases continuously with strain [17]. In particular in cold deformed austenitic stainless steels H_c seems to be mainly affected by the average size and distance of α'-martensite. After low plastic deformation low amount of α'-martensite small particles is uniformly distributed in austenitic paramagnetic grains and the distance between the ferromagnetic phases is very high. Increasing strain rate the small martensitic ferromagnetic particles form clusters and finally martensitic islands in austenitic matrix. Martensitic particles, clusters, and islands act as small ferromagnets and are magnetized when an external magnetic field is applied, influencing the magnetic properties of the material. In this way in order to reach saturation magnetic polarization and to obtain H_c value a high applied magnetic field is needed to overcome the internal demagnetization field.

In the first stage of deformation when the size of the martensitic clusters is small and the distance between them is high weak intercluster exchange interactions take place. Increasing the sizes of clusters, all the volume of the material is subjected to domain wall movement, being possible intercluster exchange interaction. The movement of domain wall is here affected by grain boundaries and defects present in the material. When the clustering size is relatively high the distance between clusters becomes more important, with important consequences on coercivity. The maximum value of coercivity is reached with quite high clustering size with strong exchange interaction over longer range than cluster size. On the contrary if the clusters are closer the grain boundaries reduce, leading to less pinning effect which causes a decrease in the coercivity [17].

In this study metastable paramagnetic austenitic phase evolved into ferromagnetic α'-martensite in a ferromagnetic

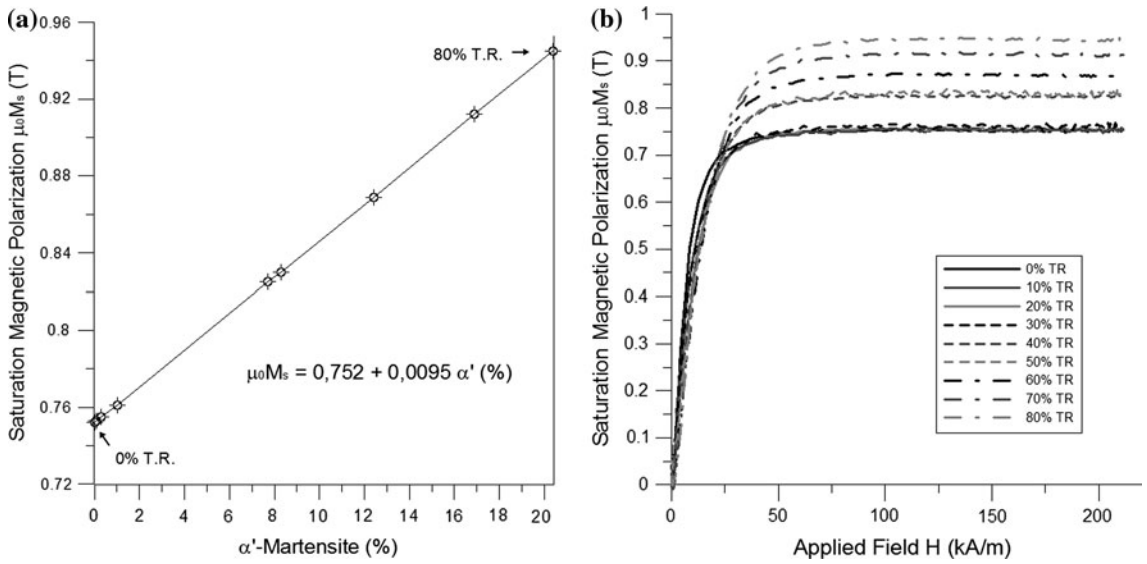

Fig. 6 **a** α'-Martensite quantification, **b** saturation magnetization curves

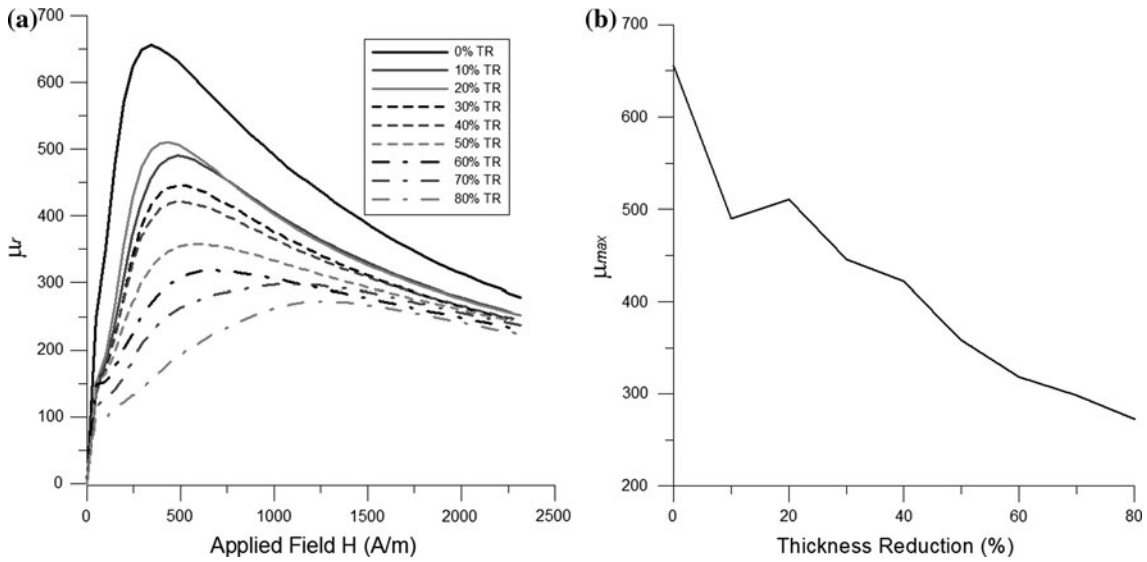

Fig. 7 **a** Relative magnetic permeability, **b** relation between maximum relative magnetic permeability and thickness reduction

ferritic matrix after cold rolling. The difference between the two matrices in which martensitic particles nucleate and grow, paramagnetic austenitic matrix in austenitic stainless steels and ferromagnetic ferritic matrix in the duplex stainless steel considered in this study, can affect the coercivity in different ways. In the duplex stainless steel neither saturation of H_c nor continuous decreasing was detected. H_c always linearly increased with thickness reduction applied, but with different slope. The trend seems to be strongly influenced by the presence and amount of strain-induced martensite. Up to 10% of thickness reduction H_c increased because of the high dislocation density. At the first appearance of α'-martensite, 10–30% of thickness reduction, H_c continued to increase but slowly. At higher thickness reduction rates H_c showed a continuous faster increase due to the high increase in α'-martensite at such strain rates. The relationship between H_c and martensite amount is plotted in Fig. 9. The strongly deformed structure, the hardening of ferritic phase, the high refining with the creation of new grain boundaries due to the different deformation feature between ferrite and the parent austenitic grains are all defects with pinning effect to domain growth and wall movements, those can help to increase H_c.

In the lean duplex stainless steel investigated in this study a strong dependence between coercivity and α'-martensite content has been highlighted. Hence, coercivity measurements may be used as a non-destructive

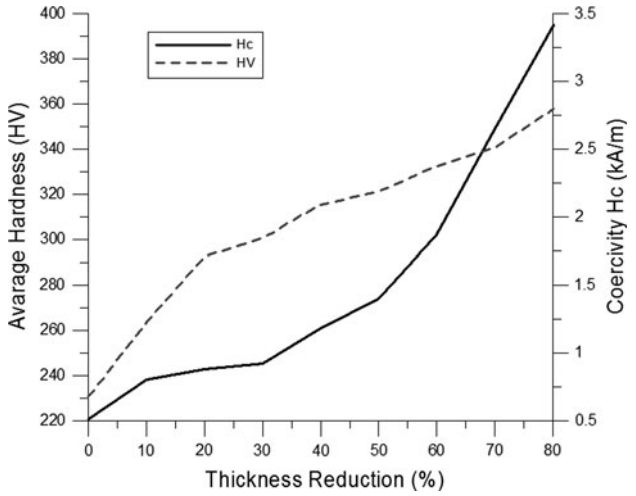

Fig. 8 Relation among vickers hardness, coercivity, and thickness reduction

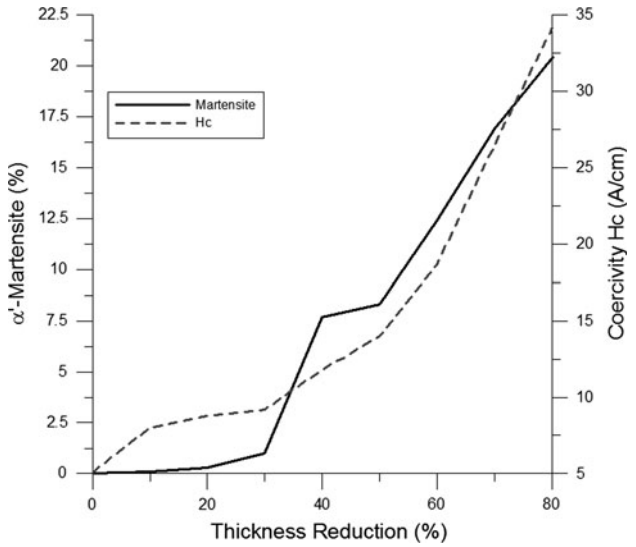

Fig. 9 Relation between coercivity, α'-martensite amount, and thickness reduction

method for useful indication of deformation-induced martensite amount for this type of steel.

Conclusions

This article concerns with the possibility to obtain a ferritic–martensitic structure in a lean ferritic–austenitic stainless steel by the application of cold deformation-inducing martensitic transformation.

Microstructural evolution occurring in a lean duplex stainless steel cold rolled in a range of 0–80% of applied thickness reduction was investigated. The results obtained can be summarized in the following conclusions.

- A strong grain refining is noticeable increasing the strain value to the maximum considered in this study, leading to grains characterized by few micrometers size.
- A practically complete ferritic–α'-martensitic structure can be obtained at 80% of applied thickness reduction.
- The presence of ferromagnetic strain-induced martensite was detected by saturation magnetic polarization measurements, and quantified by the same technique on the basis of XRD results.
- The saturation magnetic polarization seems to be not affected by cold rolling up to 30% of thickness reduction, while further increase in cold deformation lead to an increase in saturation magnetic polarization reaching the highest value of 0.94 T for the highest thickness reduction imposed (80%).
- AC magnetic results reveal an inverse ratio between derived relative permeability and cold deformation at low applied external field. Also a strong dependence between coercivity and α'-martensite content has been highlighted.
- The reciprocal of maximum relative magnetic permeability and coercivity was found to be useful parameters for non-destructive quantitative measurements of the amount of deformation-induced martensite amount in the type of steel considered.
- Both Vickers hardness and coercivity linearly increase with cold deformation.

Acknowledgements The authors acknowledge Acciaieria Valbruna S.p.a. for the furniture of the material and G. Fassina for the experimental contribution to this research. This study was partially supported by the Hungarian Research Project OTKA 80173CK.

References

1. Hayden HW, Floreen S (1970) Metall Trans 1:1955
2. Tavares SSM, Neto JM, Da Silva MR, Vasconcelos IF, Abreu HFG (2008) Mater Charact 59:901
3. Mangonon PL, Thomas G (1970) Metall Trans 1:1577
4. Milad M, Zreiba N, Elhalouani F, Baradai C (2008) J Mater Process Technol 203:80
5. Mészáros I, Prohászka J (2005) J Mater Process Technol 161:162
6. Choi JY, Jin W (1997) Scr Mater 36:99
7. Seetharaman V, Krishnan P (1981) J Mater Sci 16:523. doi: 10.1007/BF00738646
8. Baeva M, Neov S, Sonntag R (1995) Scr Metall Mater 32:1031
9. Güler E, Kirindi T, Aktas H (2007) J Alloys Compd 440:168
10. Tavares SSM, Da Silva MR, Pardal JM, Abreu HFG, Gomes AM (2006) J Mater Process Technol 180:318
11. Liljas M, Johansson P, Liu HP, Olsson COA (2008) Steel Res Int 79:466
12. Zhang L, Jiang Y, Deng B, Zhang W, Xu J, Li J (2009) Mater Charact 60:1522
13. Webb CE (1936) Rep Prog Phys 3:227

14. Vértesy G, Mészáros I, Tomás I (2005) J Magn Magn Mater 285:335
15. Baudouin P, Houbaert Y (2002) J Magn Magn Mater 246:247
16. Kronmüller H, Fähnle M (2003) Micromagnetism and the microstructure of ferromagnetic solids. Cambridge University Press, Cambridge
17. Zhang L, Takahashi S, Kamada Y, Kikuchi H, Ara K, Sato M, Tsukada T (2005) J Mater Sci 40:2709. doi:10.1007/s10853-005-2112-7
18. Mitra A, Srivastava PK, De PK, Bhattacharya DK, Jile DC (2004) Met Trans 35A:599